Effect of magnetic islands on the local plasma behavior in a tokamak experiment

E. D. Taylor,[a] C. Cates, M. E. Mauel, D. A. Maurer, D. Nadle, G. A. Navratil, and M. Shilov
Department of Applied Physics and Applied Mathematics, Columbia University, New York, New York 10027

Experiments provide simultaneous, local measurements of the pressure and ion velocity perturbations from rotating $m/n = 2/1$ magnetic islands using Mach probes in a tokamak. Measurements were made both inside and around the islands. Pressure perturbations followed the magnetic island motion for both naturally rotating and actively controlled islands. The toroidal ion velocity profile was sharply peaked near the center of the 2/1 magnetic island, and the magnitude of this peak was $\sim30\%$ of the magnetic island velocity. Active rotation control experiments also successfully changed the ion fluid velocity. The acceleration of the ion fluid was $\sim20\%$ of that experienced by the magnetic islands. Understanding the effect of magnetic islands on the pressure and ion velocity profiles is crucial for both fundamental plasma studies and the development of more efficient tokamak using advanced tokamak concepts. © *2002 American Institute of Physics.* [DOI: 10.1063/1.1499715]

I. INTRODUCTION

One of the major limitations on the performance of fusion devices is the presence of plasma instabilities. Magnetic islands are a particularly important limiting instability in the performance of a wide range of tokamaks.[1] These islands alter the overall magnetic field topology, degrading the plasma confinement. This degradation can lead to both disruptions and increased plasma transport far above the collisionally driven transport levels. Magnetic islands are not confined solely to tokamaks. Islands have also been measured in stellarators[2] and reverse-field pinches (RFPs).[3] The elimination of the islands may require an active control technique to suppress the instability during the plasma discharge.

One suppression technique of considerable interest is active rotation control.[4–8] Magnetic islands in fusion devices generally rotate at the kilohertz range of frequencies. The island rotation interacts with the background plasma to produce rotating perturbations in the plasma pressure and velocity profiles. Active rotation control attempts to use this interaction to produce damping forces in order to induce a reduction in the island size.[8–10] Understanding how the magnetic islands interact with the plasma, particularly with the ion fluid velocity, is crucial to understanding and improving rotation control techniques.

Experiments have measured the effect of magnetic islands on the ion fluid velocity. Experiments in the Doublet-IIID (DIII-D)[11,12] and Joint European Torus (JET)[13] tokamaks studied the effect of static magnetic perturbations on the ion velocity, observing a cessation of ion motion. These results suggested that the ion fluid moves together with the magnetic islands. However, work on Ohmically heated tokamaks measured a difference in the velocity and acceleration between the magnetic islands and the ion fluid. The Compact Assembly-C (COMPASS-C)[14] and JAERI (Japan Atomic Energy Research Institute) Fusion Torus–2M (JFT-2M)[15] tokamaks measured the separate motion of the ion fluid and magnetic islands during active rotation control experiments.

The COMPASS-C experiment used a system of external coils to produce a stationary 2/1 magnetic island.[14] The appearance of this stationary island reduced the ion velocity at the $q \sim 2$ surface by -7 kHz. However, natural 2/1 islands rotated at about 14 kHz, which would correspond to a change in the island velocity of -14 kHz. Hender attempted to explain this difference by attributing it to either a large shear in the velocity profile creating erroneous ion velocity measurements, or that the island flattened the pressure profile which would reduce diamagnetic velocity.

The JFT-2M tokamak observed similar behavior during active rotation control experiments.[15] Frequency ramp resonant magnetic perturbations succeeded in changing both the magnetic island and ion velocities. However, the acceleration experienced by the island was three times larger than that experienced by the ion fluid. One explanation offered suggested that the "no-slip" condition between the island and the plasma might not always hold, which is possible if pressure gradients and/or neutral damping are present.

The complex island perturbation behavior highlights the need for detailed experimental measurements. In particular, the velocity difference between the ion fluid and the magnetic island raises the question of how the pressure perturbations behave in such circumstances. Since the magnetic islands produce changes in both the ion velocity and pressure profiles, studies would need to include simultaneous measurements of both the pressure perturbation and ion velocity. These results could then provide the experimental data necessary to design and evaluate models of the interaction between magnetic islands and the plasma. The experimental

---

[a]Present address: Eaton Corporation, Vacuum Interrupter Technology Dept., Horseheads, NY 14845; electronic mail: erikdtaylor@eaton.com

TABLE I. Plasma parameters for HBT–EP.

Major radius R	94 cm
Minor radius a	13 cm
Plasma current I_p	14 kA
Toroidal field B_T	0.34 T
Pulse length	8–10 ms
Peak electron temperature T_e	150 eV
Plasma density n_e	6×10^{18} l/m^3

work on the HBT–EP (High Beta Tokamak–Extended Pulse) tokamak fills this need by simultaneously measuring the magnetic island motion, ion fluid velocity, and pressure perturbation inside and around 2/1 magnetic islands in an Ohmically heated tokamak.

II. EXPERIMENTAL DESIGN

The HBT–EP (High Beta Tokamak–Extended Pulse) tokamak is an experiment studying the behavior and control of instabilities relevant to magnetic fusion.[4,5] Table I lists some key parameters of this experiment. The experiment uses an array of diagnostics and an active rotation control system to study the behavior of magnetic islands. In particular, Mach probes made extensive measurements of the pressure and velocity perturbations due to the magnetic islands.

The key features for the study of magnetic islands on HBT–EP were the diagnostics and the external rotation control system. Magnetic islands create distinct perturbations in the magnetic field, with each type of island (2/1, 3/2, 3/1, etc.) possessing its own signature. This signature allows for the external detection of the internal island.[16] In addition, the magnetic island structure resonantly interacts with external fields with the same structure. This allows the external control of the island velocity by imposing a rotating resonant magnetic perturbation (RMP) on the plasma.[4,5]

Although Langmuir and Mach probes can provide a wealth of critical information on plasmas,[17] the application of these diagnostics to tokamaks has largely focused on the edge plasma in tokamak experiments.[18–21] The two main experimental difficulties are the perturbation of the overall plasma behavior and melting of the probes. The probe system on HBT–EP overcame the perturbation issue by reducing the probe dimensions, and by using two probes at separate locations to measure the local perturbation from probe insertion. The melting problem was managed through the careful selection of material for the probe tip and electrode materials.[22]

The Mach probe is a directional version of the Langmuir probe measuring the ratio of the ion velocity to the plasma sound speed. The electrode of the Langmuir probe is cut in half, separated by an insulator, and oriented orthogonal to the flow to produce an upstream and downstream electrode. This separation provides the directionality necessary to measure the velocity. The velocity is calculated using a theory developed by Hutchinson for the ion saturation current measured by probes in a strong magnetic field.[23] This theory models
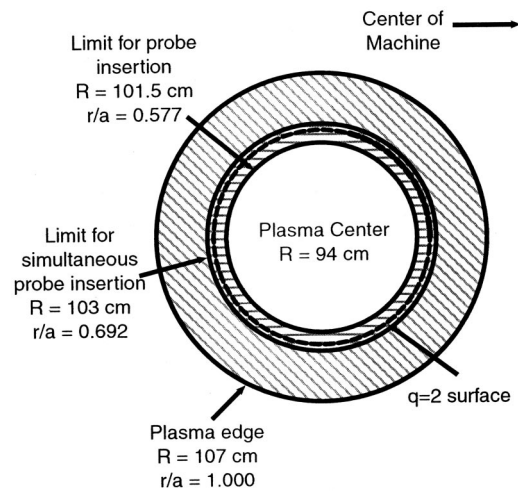

FIG. 1. Poloidal cross-section illustrating the limits of probe insertion. R is the outboard major radius, r is the minor radius, and a is the minor radius of the plasma edge. Probe was inserted from the outboard side.

the flow along the magnetic field, which in a tokamak is effectively the toroidal direction. The formula is

$$M = \frac{\nu}{c_s} = \frac{1}{2} \log\left(\frac{I_{\text{up}}}{I_{\text{down}}}\right), \tag{1}$$

where M is the Mach number, ν is the ion velocity, I_{up} and I_{down} are the ion saturation currents for the up and down stream probes, respectively, and c_s is the ion sound speed. Since the Mach probe is a Langmuir probe cut in half, it is reasonable to expect that adding both the side probe signals together will reproduce the single probe behavior. The mean of the up and down stream electrode currents demonstrate little dependence on the Mach number, and reproduce the ion saturation current formula.[23]

Experiments in the KAIST (Korea Advanced Institute of Science and Technology) tokamak reproduced the logarithmic relationship between the ion velocity and ratio of the ion saturation currents.[24] Other theories exist for the interpretation of Mach probe signals, most notably the theory developed by Stangeby.[25] The paper by Peterson summarizes and compares several of these models.[26] However, the difference between the theories is significant only at large Mach numbers. For the typical range of Mach numbers on HBT–EP, the models converge.

The effect of the probes on the global and local plasma behavior determined their insertion limits. The presence of two separate probes allowed for the independent verification of the measurements, as well as the quantification of the local plasma perturbation from the probe.[22] For $r/a > 0.692$, the location of the second probe produced no change in the other probe signal. The limit on insertion due to probe arcing was $r/a = 0.577$. The probe limits are plotted in Fig. 1. One of the probes could be rotated about its long axis between shots to verify the directionality of the measurements. For magnetic island studies, key plasma parameters were held constant between the different shots. The plasma current, major radial position, edge q, loop voltage, $m = 2$ and m
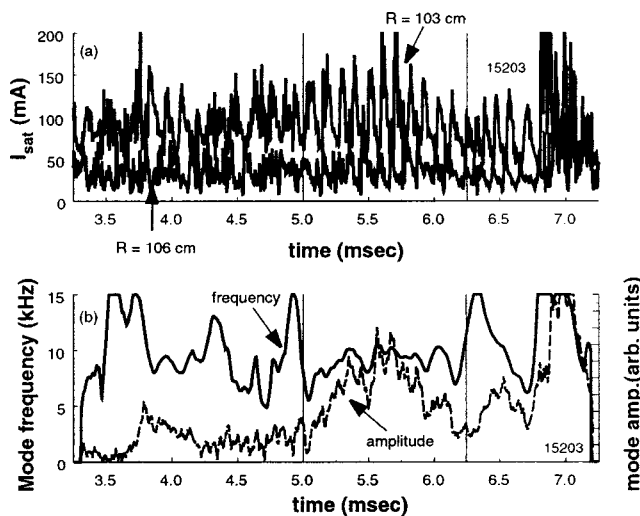
FIG. 2. Graph (a) plots effect of magnetic island activity on the ion saturation current at $r/a = 0.7$ ($R = 103$ cm) and $r/a = 0.9$ ($R = 106$ cm). Graph (b) displays the magnetic island frequency and amplitude evolution for the $m/n = 2/1$ island during this period.
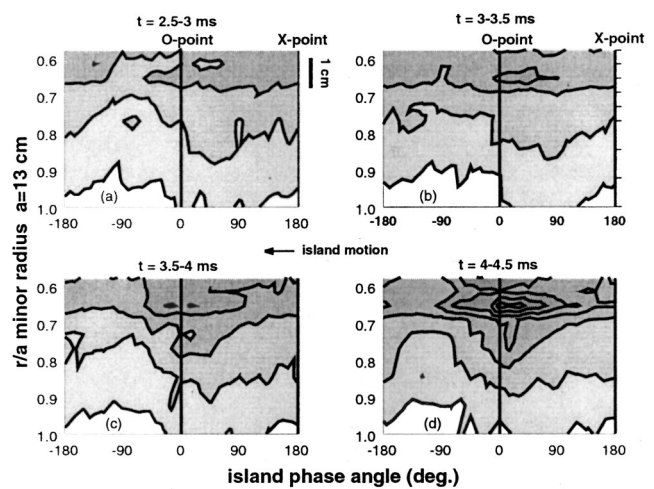

FIG. 3. Contour plots illustrating the effect of 2/1 magnetic island growth on the ion saturation current. Contours of ion saturation current are plotted against the minor radius ($r/a = 1$ is the outer plasma edge) and the phase angle relative to the magnetic O point ($0°$ is the O point, $180°$ is the X point). The island is growing in graphs (a)–(c) and reached the saturation level in (d).

$= 3$ fluctuations, line integrated density, and central soft x-ray emissions were similar for the discharges.

III. ISLAND PRESSURE PERTURBATIONS

Magnetic island rotation creates rotating perturbations in the magnetic field, density, and temperature.[2,19,27–33] Understanding the behavior of these perturbations is critical to understanding the interaction between the magnetic island and the plasma. The time evolution of the amplitude and frequency necessitates the use of a nonstationary signal analysis technique based on the Hilbert transform in order to capture the island dynamics.[34] The Hilbert transform calculated the amplitude, phase and frequency of the island signal from a single detector. Other techniques normally require systems of multiple detectors. The amplitude and frequency information helped determine the success of active rotation control techniques in both changing the island motion and reducing its magnitude. The phase information allowed the straightforward comparison of diagnostics at different physical locations and measuring different plasma properties. Knowledge of the phase also allowed the conversion of the stationary diagnostic measurements to a frame of reference co-rotating with the magnetic island. This enabled the straightforward comparison of experimental results to theoretical predictions. The Hilbert transform method compares favorably both in speed and accuracy to spectrogram and quadrature methods of spectral calculations.

Ion saturation current measurements on HBT–EP demonstrated the effect of magnetic islands on the pressure profile. The first step in this analysis was to connect probe fluctuations to magnetic island activity. The fluctuations in the ion saturation current are both localized near the island and follow its amplitude evolution. Figure 2 plots the ion saturation current measured at two different major radial positions in the same shot, one at $r/a = 0.7$ and the second closer to the edge at $r/a = 0.9$. Figure 2 also shows the magnetic island frequency and amplitude evolution. During the early portion

of the shot, the probes observe high frequency oscillations with little coherent structure. As the magnetic island amplitude increases at $t \sim 5$ ms the probe begins to detect coherent fluctuations at $r/a = 0.7$. These fluctuations follow the evolution of the island amplitude from $t \sim 5 - 6.25$ ms. The probe at $r/a \sim 0.9$ does not measure fluctuations until later in the shot at $t \sim 6$ ms when the island amplitude is large. These results show that the fluctuations in the ion saturation current follow the magnetic island amplitude behavior and are spatially localized inside the plasma. Voltage scans of the probes suggested that the ion saturation current perturbation is largely an increase in the local density.[22]

The radial profile of the pressure perturbation can be converted into a frame corotating with the magnetic island using the phase values calculated with the Hilbert transform.[34] This analysis generated contour plots of the time evolution of the magnetic island as a two-dimensional function of the phase angle relative to the magnetic perturbation peak and the minor radius. This method allows comparison to magnetic island theories, which often state results in either the island frame of reference or in one where the electric field vanishes. In particular, theories and experiments tend to focus on the O and X point behavior. The toroidal rotation of the island past the stationary probe produces a toroidal scan of the magnetic island. Data in 0.5 ms intervals were sorted by angle then averaged in intervals of $15°$. Each angle corresponds to a toroidal location corotating with the magnetic island.

Figures 3 and 4 contain contour plots of the ion saturation current versus the minor radius and phase angle relative to the magnetic island O point from $t = 3 - 7$ ms. Early in the shot the small magnetic island makes a small perturbation centered at $r/a = 0.654$. As the island grows in amplitude during $t = 4 - 5$ ms, the size and extent of the perturbation increases. Once the island saturates during $t = 5 - 7$ ms, the perturbation remains constant.
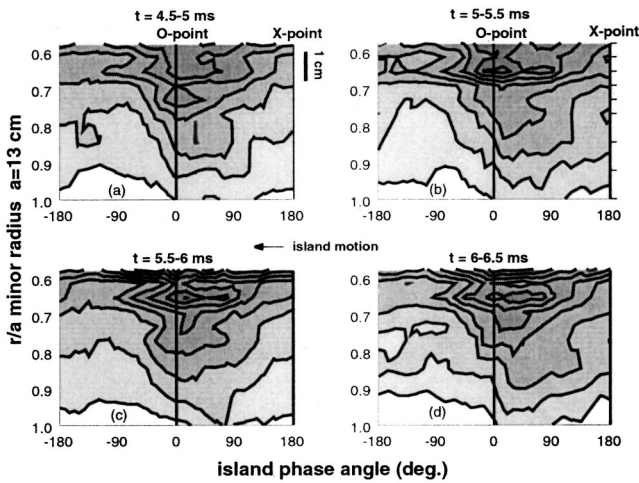
FIG. 4. Same as Fig. 3 for later times when the 2/1 magnetic island is saturated. The saturated island width extended over the 1 cm regions from $r/a \approx 0.615 - 0.692$.

FIG. 6. Ion velocity as a function of minor radius. Cross-hatched region indicates the location of the 2/1 magnetic island.

These contour plots illustrate several key behaviors of the magnetic islands. The ion saturation current perturbation is centered at the island O-point at a minor radius of $r/a = 0.654$. The pressure perturbation decays both radially and toroidally from the island O point. The size and extent of the perturbation both follow the behavior of the magnetic perturbation, featuring a small perturbation that grows over a 1 ms period and then saturates at a constant magnitude. The dominant perturbation occurred over a 1 cm region extending from $r/a \approx 0.615 - 0.692$. This size agrees with estimates of the magnetic island size from magnetic measurements based on the island width equation

$$W = 4 \left(\frac{r q B_r}{m q' B_p} \right)^{1/2} \approx 1 \quad \text{cm}, \tag{2}$$

where W is the magnetic island width, r is the minor radius of the island, q is the safety factor, B_r is the magnitude of the magnetic perturbation from the island, m is the mode number, q' is the local shear in q, and B_p is the poloidal field strength.[35] The perturbation was not exclusively confined to the estimated island width of 1 cm, but appeared to some degree over the entire outer minor radius.

Further information about the perturbation can be acquired by focusing on the behavior of the O and X points of the magnetic island (Fig. 5). Early in time at $t = 2.5 - 3$ ms

there is little difference between the O and X point radial profiles, as expected for small island sizes. When the island has saturated at $t = 5.5 - 6$ ms, the perturbation at the O point increased in magnitude from the magnetic island region out to the plasma edge. A flat region existed at the center of the perturbation at $r/a = 0.654$ from the local peak in the ion saturation current. The X point profile remains unchanged by the island growth. This behavior suggests that the pressure perturbation was largely confined to the region near the O point.

IV. ION VELOCITY MEASUREMENTS

Local measurements of the ion fluid both inside and around the 2/1 magnetic islands using the Mach probe system made two key velocity observations on the HBT–EP tokamak. First, the ion velocity profile had a large peak located near the center of the 2/1 magnetic island. Figure 6 plots the radial profile of the toroidal ion velocity. A large peak in the velocity profile occurs at the location of the 2/1 magnetic island. Second, the ion velocity at this peak was significantly lower than the magnetic island velocity. HBT–EP observed similar velocity behavior as seen on the COMPASS-C[14] and JFT-2M tokamaks.[15] Figure 7 compares the velocity of the 2/1 magnetic island and the local ion fluid at the island, observing a factor of 3 difference between the velocities.
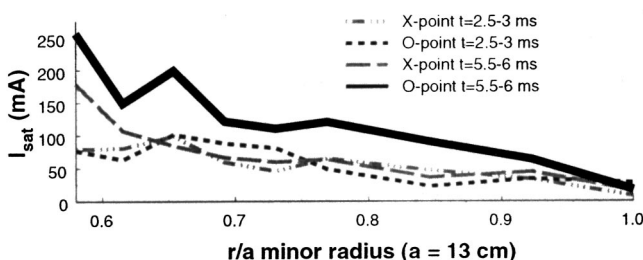

FIG. 5. Ion saturation current as a function of the minor radius plotted at the O and X points of a small 2/1 magnetic island from Fig. 3(a), and for a saturated island from Fig. 4(c).
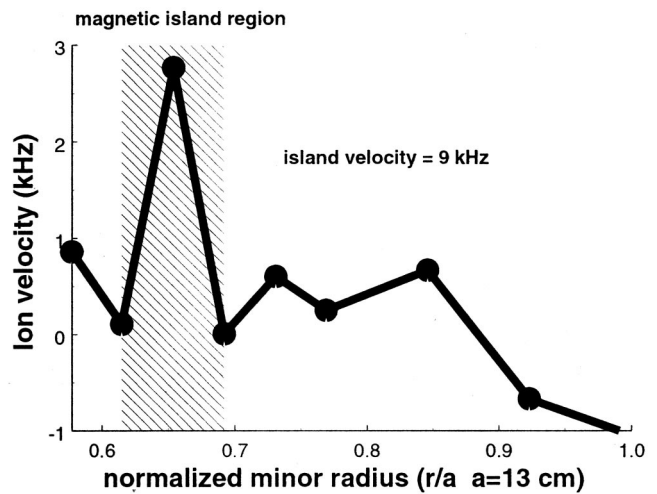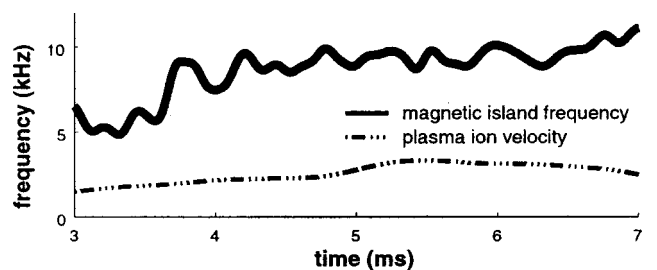

FIG. 7. Comparison of the 2/1 magnetic island and ion fluid velocity at the magnetic island as a function of time.
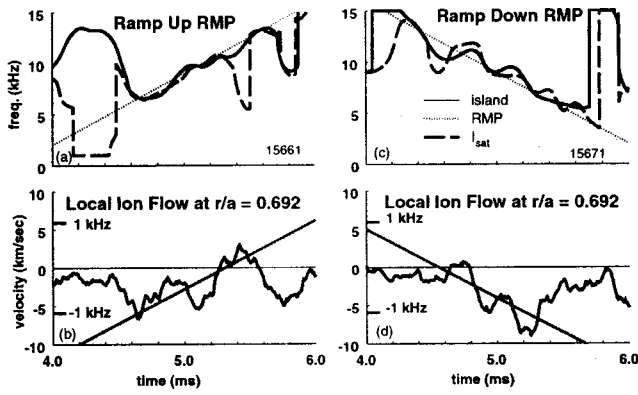
FIG. 8. Effect of active rotation on the 2/1 magnetic island, pressure perturbation, and ion velocity. (a) and (c) plot the external perturbation and the effect on the magnetic island and pressure perturbation. (b) and (d) plot the ion fluid velocity near the magnetic island. The straight lines in (b) and (d) indicate the change in the velocity during the control period.

Further experiments with active rotation control demonstrated that the acceleration experienced by the ion fluid is only 20% of that experienced by the magnetic island. Rotation control provides an external means of altering the magnetic island motion.[4–6] During frequency ramps, the frequency of the RMP (resonant magnetic perturbation) is linearly swept in time. The changing frequency of the RMP drives a changing island velocity, thereby accelerating or decelerating the island. Figures 8(a) and 8(c) plot the frequencies of the RMP used for rotation control, the magnetic island, and the fluctuations in the ion saturation current. The pressure perturbation followed changes in the island frequency, with the island and pressure perturbation frequencies equal during the rotation control. Rotation control also successfully changed the ion fluid velocity [Figs. 8(b) and 8(d)]. However, both the velocity and acceleration of the ions were less than that of the magnetic island, with the ion fluid acceleration being only 20% of the magnetic island acceleration.

V. EXPERIMENTAL MODELING

Two interesting features emerge from the ion fluid velocity measurements. First, the ion velocity is less than that of the 2/1 magnetic island, as shown in Fig. 7. Second, the ion velocity is peaked within the magnetic island, as shown in Fig. 6. Both these features are consistent with standard neoclassical theory[36] when combined with two simplifying assumptions. The first assumption is that the magnetic island moves with the electron fluid. Standard neoclassical theory decomposes the electron and ion flows into field-aligned and toroidal components. Since the field-aligned flows do not create an observable frequency, the first assumption implies the frequency of the magnetic island is proportional to n/R times the toroidal electron flow. The island frequency, ω_{island}, is equal to the toroidal mode number, n, times the sum of the $\mathbf{E} \times \mathbf{B}$ and electron diamagnetic frequencies. The second assumption is that the ion flow is reduced significantly by interactions with neutral particles. The ion flow is forced to nearly vanish in the laboratory frame of reference. Since the ion diamagnetic frequency is directed oppositely

from the electrons, the neutral drag on the ions force the $\mathbf{E} \times \mathbf{B}$ flow to be in the electron diamagnetic drift direction, and this further increases the natural frequency of the magnetic island.

Analyses of measurements of the magnetic island motion in the ASDEX[32] and COMPASS-C[14] tokamaks support the first assumption. In each case, the observed frequency of the magnetic island is similar to the toroidal rotation velocity of the electron fluid, $\omega_{island} \approx n\omega_e$. In tokamaks, the variation in the strength of the toroidal magnetic field with major radius dampens the plasma flow in the poloidal direction.[37] Two flux functions, the field-aligned flow and the toroidal flow can describe the mass flow. In neoclassical theory, the field-aligned flow is the poloidal flow and is strongly damped, leaving only the toroidal component.[37,38] This sharply increases the predicted toroidal velocity magnitude according to the relation[32,39]

$$\nu_T \sim \nu_\parallel = \frac{B_T}{B_P} \cdot \nu_\perp , \tag{3}$$

where ν_T is the toroidal velocity, $\nu_\parallel$ is the velocity parallel to the magnetic field, B_T and B_P are the toroidal and poloidal magnetic fields. Based on this damping, the diamagnetic term for the ions ω_{*i} is

$$\omega_{*i} = \frac{1}{2\pi R} \frac{\nabla p_i}{q_i n B_p}, \tag{4}$$

where ∇p_i is the ion pressure gradient, R is the major radius, q_i is the ion charge, and n is the plasma density. There is a similar expression for the electron diamagnetic frequency, ω_{*e}.

Although the ion and electron fluid flows are sensitive to the pressure gradient, the observed island frequency is probably independent of the diamagnetic flows. This is because the pressure gradient, and hence the diamagnetic frequency, go to zero within the magnetic island. Theoretical models suggested that the profile changes from magnetic islands alter the diamagnetic velocity.[40–42] A two-fluid simulation of the effect of magnetic islands on the pressure calculated that the gradient inside the magnetic island would decay to near zero, $\nabla p \sim 0$, on the order of $\tau_R/10$, a tenth of the resistive time scale. For HBT–EP, this time is ~ 0.45 ms, or approximately 1/16 of the plasma shot length. Finn also performed a two-fluid plasma simulation demonstrating that magnetic islands alter the pressure profile, which in turn changed the diamagnetic velocity and hence the ion velocity. These simulations differed, however, on the extent of the pressure flattening. In the Scott simulation the pressure flattened over the entire magnetic island once the island was larger than the critical width for sound flattening, which for HBT–EP is $W_{sound} \sim 2.4$ cm. Finn determined that the flattening was a function of ratio of the ion sound speed to the Alfvén speed for the propagation of magnetic fluctuations. For HBT–EP, this ratio is

$$\frac{c_S}{\nu_{Alfvén}} \sim 0.03 . \tag{5}$$

This value corresponds to a reduction of the pressure gradient over only a portion of the island. Fitzpatrick determined a similar result using a diffusion-based model for the flattening of the temperature and density profiles. Tokamaks the size of HBT–EP would not expect complete flattening of the density profile inside the magnetic island until the width is greater than the critical width $W_{dens} \sim 3$ cm. Temperature profile flattening was predicted for islands larger than $W_{temp} \sim 0.8$ cm. These differing expectations necessitate the measurement of both the pressure perturbations from the magnetic island, and the effect on the ion velocity profile. Although a region with $\nabla p \sim 0$ is observed in Fig. 5 at the O point, the behavior differs from flattening models. The O point perturbation increases the ion saturation current in particular over the magnetic island region, but also over the rest of the outer radius of the plasma, extending to the plasma edge.

The second assumption is that charge exchange reactions between the ion fluid and neutral gas atoms dampen the ion flow. Experiments on the TEXT (Texas Experimental Tokamak) experiment determined that the inclusion of neutral damping and diamagnetic effects allowed the successful prediction of the ion velocity profile.[43] The charge exchange removes the ion momentum from the system and introduces a new stationary ion. The model reduces the ion velocity by a factor F_{cx},

$$\omega_i = F_{cx} \omega_{i \text{ No cx}} = F_{cx}(\omega_E - \omega_{*i}). \tag{6}$$

F_{cx} ranges in value from $0 \leq F_{cx} \leq 1$, where one corresponds to no effect from the neutrals, and zero corresponds to the complete suppression of the flow (from high neutral densities).

Combining these two assumptions allows for the modeling of the ion velocity behavior observed in HBT–EP. Pressure flattening at the magnetic island allows the estimation of the neutral damping term F_{cx} at the magnetic island. When the pressure gradient is zero, the diamagnetic term is zero, $\omega_{*i} \sim 0$, which reduces the velocity equation to

$$\omega_i = F_{cx} \omega_E. \tag{7}$$

For a 2/1 magnetic island with $n=1$, the electron velocity equation reduces to

$$\omega_e = \omega_{island} = \omega_E. \tag{8}$$

The ratio of the two gives

$$\frac{\omega_i}{\omega_e} = F_{cx}. \tag{9}$$

Magnetic island velocity measurements determine the electron velocity and $\mathbf{E} \times \mathbf{B}$ flow at the island location. This value, combined with the ion velocity, gives the neutral damping term at the magnetic island as

$$F_{cx} \approx 31\%. \tag{10}$$

The diamagnetic and neutral damping terms can be combined with measurements of ω_i to solve Eq. (6) for the ω_E term. The diamagnetic term is estimated based on the ion saturation current measurements of the probe system. Figure 9(a) plots ω_i, $F_{cx}\omega_E$, and $-F_{cx}\omega_{*i}$ as functions of the nor-
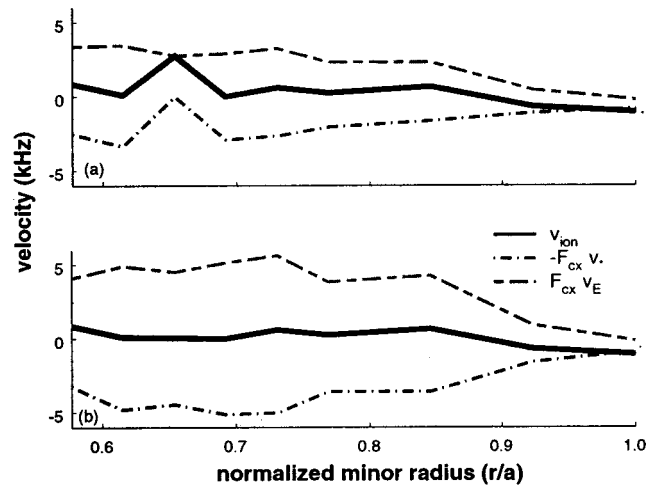

FIG. 9. The diamagnetic, electric field, and neutral damping contributions to the ion velocity as functions of the minor radius. (a) includes the pressure and velocity perturbations from the 2/1 island, and (b) is with these perturbations removed.

malized minor radius. The large peak in the ion velocity is readily attributed to the elimination of the diamagnetic term inside the magnetic island. The neutral damping reduced the overall magnitude of the velocity terms. Examining the velocity profiles in the absence of the magnetic island further highlights the importance of the islands in determining the ion velocity profile. The pressure perturbation due to the magnetic island is confined largely to the magnetic O point. Thus, the X point corresponds to the unperturbed pressure profile and can be used to calculate ω_{*i} without the island. The perturbation in the ion velocity is eliminated by replacing the peak at $r/a = 0.654$ with the interpolated value from the surrounding data points. Figure 9(b) shows ω_i, $F_{cx}\omega_E$, and $-F_{cx}\omega_{*i}$ with the island perturbations in the pressure and velocity removed. The electric field and diamagnetic terms outside the island region are similar to the previous case. The key effect of the magnetic island is to locally flatten the velocity profile, eliminating the local diamagnetic velocity. This creates a distinct, local increase in the ion fluid velocity.

When the diamagnetic term goes to zero, the ion fluid moves at $F_{cx}\omega_E$, the electric field velocity multiplied by the neutral damping term. This behavior agrees with two-fluid simulations that predict pressure flattening inside the island.[40] This flattening leads to the dominance of the electric field term in the velocity equation. The limited radial extent of the velocity perturbation agrees with predictions of limited pressure profile flattening for plasma parameters typical of HBT–EP.[41,42] This model suggests that magnetic islands produce distinct, localized perturbations in the ion velocity that are consistent with changes in the diamagnetic velocity term in the presence of poloidal flow damping, and assuming that the electric field is unperturbed by the presence of the magnetic island. Furthermore, the presence of charge exchanging damping of the ion flow could potentially explain the reduced velocity and acceleration of the ion fluid as compared to that of the 2/1 magnetic island (Fig. 8).

VI. DISCUSSION

The measurement of the pressure perturbations from magnetic islands on HBT–EP extends the range of previous probe experiments. The ability to measure minor radial positions from $0.577 \leq r/a \leq 1.0$ substantially expands the range of observation. Previously, measurements of pressure perturbations from islands with probes were confined to the edge region of tokamaks.[19] Most other probe systems focused on turbulence measurements at the edge of different devices.[18,44,45]

Application of the Hilbert transform to convert the data to a co-rotating frame complements multichord and multipoint measurements of the pressure perturbation. This novel application of the transform enabled a single probe to reproduce results similar to electron cyclotron emissions (ECE) and other multiple detector diagnostic systems.[27–30,33] The phase information allowed the reconstruction of the magnetic island perturbation with a single moveable diagnostic and a reasonable number of plasma shots.[34] This can be compared to ECE, which requires a large number of expensive detectors. This feature could translate into significant cost and design savings, and encourage more research into the use of moveable detectors for magnetic island studies. It also increases the usefulness of probes in island studies by reducing the size of the probe required to track the pressure and velocity effects.[21] Finally, the Hilbert transform can serve as the basis for improved island analysis methods. The success of its application to rotation control studies will hopefully drive the development of new methods for applications where the Hilbert transform assumptions are not met, particularly for island locking and stationary perturbation studies.

Ion velocity measurements determined that the ion fluid and magnetic islands have different velocities, as well as different accelerations under rotation control. The ion velocity profile is peaked at the island, with this peak velocity being less that the magnetic island velocity. This behavior is consistent with a two-fluid model that includes diamagnetic and neutral damping effects. Pressure flattening inside the magnetic island could reduce the diamagnetic velocity term, increasing the ion velocity. The radial extent of this velocity perturbation is equal to or smaller than the magnetic island size, in agreement with theories predicting pressure flattening over only a portion of the magnetic island.[40–42] Neutral damping may account for the difference between the ion fluid and magnetic island velocities.[43] The combination of diamagnetism and neutral damping may help explain the complex velocity behavior observed on HBT–EP, and offers the potential to explain the ion fluid and island motion observed on COMPASS-C[14] and JFT-2M.[15]

The interaction between the magnetic island and the plasma highlight the need for further measurements of the effect of islands on the pressure and velocity profiles. Measurements of the effect of the island at the O and X points have determined different results on different machines.[2,27,28,30] This behavior highlights the need to measure, rather than simply assume, what effect the island has on the pressure profile. Velocity measurements suggest the interaction between the island and pressure profile can in turn alter the ion velocity. These factors highlight the need for models that combine the effects of the islands on both the pressure and velocity profiles.[41]

Understanding the effect of magnetic islands on the pressure and ion velocity profiles is crucial for both fundamental plasma studies and the development of more efficient tokamaks using advanced tokamak (AT) concepts. For fundamental studies, magnetic island research can provide the means to test theories about the interaction between magnetic fields and the ion and electron fluids. AT design concepts[46,47] depend on the ability of active rotation control to suppress magnetic islands and resistive wall modes.[48] An understanding of how the magnetic islands, pressure and velocity profiles, and external control systems interact is required to insure the successful operation of new tokamak designs.

[1] O. Sauter, R. J. LaHaye, Z. Chang *et al.*, Phys. Plasmas **4**, 1654 (1997).
[2] R. Jaenicke and the W VII-A Team, Nucl. Fusion **28**, 1737 (1988).
[3] D. J. Den Hartog, J. T. Chapman, D. Craig *et al.*, Phys. Plasmas **6**, 1813 (1999).
[4] M. E. Mauel, J. Bialek, C. Cates, H. Dahi, D. Maurer, D. Nadle, G. A. Navratil, M. Shilov, and E. Taylor, *Plasma Physics and Controlled Nuclear Fusion Research 1998*, Proceedings of the 17th International Conference, Yokohama (International Atomic Energy Agency, Vienna, 1999).
[5] G. A. Navratil, C. Cates, M. E. Mauel, D. Maurer, D. Nadle, E. Taylor, Q. Xiao, W. A. Reass, and G. A. Wurden, Phys. Plasmas **5**, 1855 (1998).
[6] A. W. Morris, T. C. Hender, J. Hugill *et al.*, Phys. Rev. Lett. **64**, 1254 (1990).
[7] A. I. Smolyakov, A. Hirose, E. Lazzaro *et al.*, Phys. Plasmas **2**, 1581 (1995).
[8] G. Kurita, T. Tuda, M. Azumi, and T. Takeda, Nucl. Fusion **32**, 1899 (1992).
[9] T. H. Jensen, A. W. Leonard, and A. W. Hyatt, Phys. Fluids B **5**, 1239 (1993).
[10] M. Yokoyama, J. D. Callen, and C. C. Hegna, Nucl. Fusion **36**, 1307 (1996).
[11] R. J. LaHaye, R. J. Groebner, A. W. Hyatt, and J. T. Scoville, Nucl. Fusion **33**, 349 (1993).
[12] R. J. LaHaye, C. L. Rettig, R. J. Groebner *et al.*, Phys. Plasmas **1**, 373 (1994).
[13] J. A. Snipes, D. J. Campbell, P. S. Haynes, T. C. Hender, M. Hugon, P. J. Lomas, N. J. Lopes Cardozo, M. F. F. Nave, and F. C. Schüller, Nucl. Fusion **28**, 1085 (1988).
[14] T. C. Hender, R. Fitzpatrick, A. W. Morris *et al.*, Nucl. Fusion **32**, 2091 (1992).
[15] K. Oasa, H. Aikawa, Y. Asahi *et al.*, *Plasma Physics and Controlled Nuclear Fusion Research 1994*, Proceedings of the 15th International Conference, Seville (International Atomic Energy Agency, Vienna, 1995), Vol. 2, p. 279.
[16] I. H. Hutchinson, *Principles of Plasma Diagnostics* (Cambridge University Press, New York, 1987).
[17] N. Hershkowitz, *Plasma Diagnostics Volume 2* (Academic, New York, 1989).
[18] J. Boedo, D. Gray, L. Chousal *et al.*, Rev. Sci. Instrum. **69**, 2663 (1998).
[19] A. A. Howling and D. C. Robinson, Plasma Phys. Controlled Fusion **30**, 1863 (1988).
[20] C. S. MacLatchy, C. Boucher, D. A. Poirer *et al.*, Rev. Sci. Instrum. **63**, 3923 (1992).

[21]C. Xiao, K. K. Jain, W. Zhang, and A. Hirose, Phys. Plasmas **1**, 2291 (1994).

[22]E. D. Taylor, Ph.D. thesis, Columbia University, 2000.

[23]I. H. Hutchinson, Phys. Fluids **30**, 3777 (1987).

[24]J. C. Yang, S. H. Seo, G. C. Kwon *et al.*, Phys. Lett. A **185**, 428 (1994).

[25]P. C. Stangeby, Phys. Fluids **27**, 2699 (1984).

[26]B. J. Peterson, J. N. Talmadge, D. T. Anderson *et al.*, Rev. Sci. Instrum. **65**, 2599 (1994).

[27]P. C. deVries, G. Waidmann, A. J. H. Donne, and F. C. Schuller, Plasma Phys. Controlled Fusion **38**, 467 (1996).

[28]P. C. deVries, G. Waidmann, A. Kramer-Flecken *et al.*, Plasma Phys. Controlled Fusion **39**, 439 (1997).

[29]D. L. Brower, S. C. McCool, J. Y. Chen *et al.*, *Plasma Physics and Controlled Nuclear Fusion Research 1992*, Proceedings of the 14th International Conference (International Atomic Energy Agency, Vienna, 1993), Vol. 2, p. 177.

[30]P. Van Milligen, A. C. A. P. Van Lammeren, N. J. Lopes Cardozo *et al.*, Nucl. Fusion **33**, 1119 (1993).

[31]G. Vahala, L. Vahala, J. H. Harris *et al.*, Nucl. Fusion **20**, 17 (1980).

[32]O. Klüber, H. Zohm, H. Bruhns *et al.*, Nucl. Fusion **31**, 907 (1991).

[33]Y. Nagayama, G. Taylor, E. D. Fredrickson *et al.*, Phys. Plasmas **3**, 2631 (1996).

[34]E. D. Taylor, C. Cates, M. E. Mauel, D. A. Maurer, D. Nadle, G. A. Navratil, and M. Shilov, Rev. Sci. Instrum. **70**, 4545 (1999).

[35]G. Bateman, *MHD Instabilities* (MIT Press, Cambridge, 1978).

[36]Y. B. Kim, P. H. Diamond, and R. J. Groebner, Phys. Fluids B **3**, 2050 (1991).

[37]T. H. Stix, Phys. Fluids **16**, 1260 (1973).

[38]S. P. Hirshman and D. J. Sigmar, Nucl. Fusion **21**, 1079 (1981).

[39]P. C. deVries, Ph.D. thesis, University of Utrecht, 1997.

[40]B. D. Scott, A. B. Hassam, and J. F. Drake, Phys. Fluids **28**, 275 (1985).

[41]J. M. Finn, Phys. Plasmas **5**, 3595 (1998).

[42]R. Fitzpatrick, Phys. Plasmas **2**, 825 (1995).

[43]W. L. Rowan, A. G. Meigs, E. R. Solano *et al.*, Phys. Fluids B **5**, 2485 (1993).

[44]G. Fiskel, S. C. Prager, P. Pribyl *et al.*, Phys. Rev. Lett. **75**, 3866 (1995).

[45]K. Uehara, T. Kawakami, H. Amemiya *et al.*, Nucl. Fusion **38**, 1665 (1998).

[46]F. Najmabadi, ARIES team, *Plasma Physics and Controlled Nuclear Fusion Research 1996*, Proceedings of the 16th International Conference, Montreal (International Atomic Energy Agency, Vienna, 1997), Vol. 3, p. 383.

[47]R. D. Stambaugh, V. S. Chan, R. L. Miller *et al.*, *Plasma Physics and Controlled Nuclear Fusion Research 1996*, Proceedings of the 16th International Conference, Montreal (International Atomic Energy Agency, Vienna, 1997), Vol. 3, p. 395.

[48]A. M. Garofalo, A. D. Turnbull, E. J. Strait *et al.*, Phys. Plasmas **6**, 1893 (1999).